

# Swift heavy ion induced surface modification for tailoring coercivity in Fe–Ni based amorphous thin films

Senoy Thomas,<sup>1,a),b)</sup> Hysen Thomas,<sup>1</sup> D. K. Avasthi,<sup>2</sup> A. Tripathi,<sup>2</sup> R. V. Ramanujan,<sup>3</sup> and M. R. Anantharaman<sup>1,a),c)</sup>

<sup>1</sup>Department of Physics, Cochin University of Science and Technology, Cochin 682022, India

<sup>2</sup>Materials Science Division, Inter University Accelerator Centre, New Delhi 110067, India

<sup>3</sup>School of Materials Science and Engineering, Nanyang Technological University, Nanyang Avenue, Singapore 639798, Singapore

(Received 26 August 2008; accepted 18 December 2008; published online 10 February 2009)

Fe–Ni based amorphous thin films were prepared by thermal evaporation. These films were irradiated by 108 MeV Ag<sup>8+</sup> ions at room temperature with fluences ranging from  $1 \times 10^{12}$  to  $3 \times 10^{13}$  ions/cm<sup>2</sup> using a 15 UD Pelletron accelerator. Glancing angle x-ray diffraction studies showed that the irradiated films retain their amorphous nature. The topographical evolution of the films under swift heavy ion (SHI) bombardment was probed using atomic force microscope and it was noticed that surface roughening was taking place with ion beam irradiation. Magnetic measurements using a vibrating sample magnetometer showed that the coercivity of the films increases with an increase in the ion fluence. The observed coercivity changes are correlated with topographical evolution of the films under SHI irradiation. The ability to modify the magnetic properties via SHI irradiation could be utilized for applications in thin film magnetism. © 2009 American Institute of Physics. [DOI: 10.1063/1.3075581]

## I. INTRODUCTION

Soft magnetic alloys based on Fe–Ni are increasingly becoming a hot topic of research because of their potential in finding end uses in fields such as power electronics, sensors, and actuators.<sup>1–5</sup> The magnetic softness of these materials is attributed to the amorphous microstructure which aids in the vanishing of their magnetic anisotropies. The high electrical resistance with respect to its crystalline counterparts makes them suitable for high frequency applications. The low coercivity and high permeability exhibited by these materials have been successfully explained based on the random anisotropy characteristics of the system.<sup>6</sup>

Metallic alloys with disordered structure are produced from the liquid state during cooling and are also known as metallic glasses.<sup>7</sup> There are several methods in vogue for the preparation of amorphous alloys. Here, physical vapor deposition, high energy ball milling, ion beam irradiation, and melt spinning need special mention. With the advent of these materials exhibiting excellent soft magnetic properties, thin films of these materials assume importance from an application point of view.

Control of magnetic properties is highly essential in order to obtain miniaturized magnetic devices with improved performance characteristics. The magnetic properties are strongly dependent on the microstructure and hence the magnetic properties of these materials can be tailored by modifying the microstructure. For example, the variation in the sputtering rate during the sputter deposition of magnetic thin films can result in the modification of coercivity.<sup>8</sup> Coercivity

of magnetic thin films can also be tailored by depositing films on seed layers.<sup>9</sup> Recently we reported the modification of the magnetic properties in Fe based nanocrystalline alloys by thermal annealing.<sup>10</sup> In thin magnetic films, the surface roughness plays an important role in the magnetization reversal mechanisms and this in turn determines the coercivity of the material.<sup>11,12</sup>

Ion irradiation has been considered as an alternative tool in modifying the surface properties. An energetic ion that penetrates a solid loses energy mainly via two independent processes: (a) electronic excitation and ionization [electronic energy loss,  $(dE/dx)_e$ ] which are dominant in the high energy regime (greater than 1 MeV/nucleon) and (b) elastic collisions with nuclei of the target atoms [nuclear energy loss  $(dE/dx)_n$ ] which are dominant in the low energy regime. The ion energy loss per unit path length depends strongly on the ion velocity. Swift heavy ion (SHI) passes through a solid with a velocity comparable to the Bohr velocity of electrons and loses its energy while traversing through the material. The rapid energy transfer during the inelastic collision results in a transient excitation of the medium that finally culminates in the production of point defects, clusters, columnar defects, and phase transformation along the path of the heavy ion beam.<sup>13–17</sup>

The mechanism by which the energy can be deposited is through two different process, namely, thermal spike and Coulomb explosion.<sup>18–20</sup> In the former the ion beam excites the electronic system at the local site and electrons transfer this energy to phonons via electron-phonon coupling resulting in an increase in the local temperature. In the latter, ions create ionization zones during their passage through the material. The ionization zone with positive charges may explode under electrostatic force and induces strain in the material.

Metallic glasses were thought of resistant to irradiation

<sup>a)</sup> Author to whom correspondence should be addressed.

<sup>b)</sup> Electronic mail: senoythomas@yahoo.co.in.

<sup>c)</sup> Electronic addresses: mra@cusat.ac.in and mraiyeer@gmail.com.

induced modifications. This hypothesis was based on the fact that irradiation induced disorder is easily absorbed in the heavily disordered structure of an amorphous system. But in the 1980s it was observed that metallic glasses when subjected to irradiation produced damages.<sup>21,22</sup> Glassy alloys such as Pd<sub>80</sub>Si<sub>20</sub> and Cu<sub>50</sub>Zr<sub>50</sub> when irradiated with high energy ions were found to be undergoing dimensional changes perpendicular to the ion beam, whereas the sample shrunk in dimension parallel to the ion beam. Measurements using x-ray diffraction (XRD) and electrical resistivity revealed that the structural modifications of radiation deformed samples were small in comparison to the dimensional changes. This discovery was rather surprising because of the following: (1) At that time there was a supposition that a metallic glass, as a completely disordered metal, would be more radiation resistant than any crystalline metal. (2) In crystalline materials any radiation induced anisotropic change in sample dimensions are due to a natural crystallographic anisotropy. In sharp contrast, dimensional changes in glassy Pd<sub>80</sub>Si<sub>20</sub> and Cu<sub>50</sub>Zr<sub>50</sub> were introduced by the beam itself and (3) the number of atoms, which occupied new positions in order to accommodate the dimensional changes exceeded by one or two orders of magnitude than the number of atoms which are displaced via the nuclear energy loss.

Later on, the anisotropic growth in metallic glasses was experimentally evidenced by many researchers.<sup>23,24</sup> Audouard *et al.*<sup>23</sup> observed that the irradiation of Fe<sub>85</sub>B<sub>15</sub> ribbons with 850 MeV <sup>207</sup>Pb and 350 MeV <sup>238</sup>U ions results in the formation of hillocks and hollows. The formation of hillocks and hollows were linked to the occurrence of anisotropic growth phenomenon. Later on, FeBSiC and Fe<sub>55</sub>Zr<sub>45</sub> ribbons were subjected to investigate the role of linear rate of electronic excitation  $(dE/dx)_e$  and temperature on defect creation and growth process.<sup>24</sup> Contrary to the earlier belief that the effect of SHI on metallic glasses was limited to the anisotropic growth, Dunlop *et al.*<sup>25</sup> in 2003 showed that partial crystallization of an amorphous alloy (FINEMET) is also possible by a high level of electronic energy deposition. This crystallization phenomenon was interpreted in terms of an irradiation induced pressure wave which allowed a rearrangement of the local atomic structure of the alloy. These findings lead to the conviction that electronic excitation could induce structural modification in metallic glasses and also macroscopic variations in the dimensions of irradiated metallic glass should induce modifications of the topography of the sample surface.

Fe<sub>40</sub>Ni<sub>38</sub>Mo<sub>8</sub>B<sub>14</sub> (METGLAS 2826) is an amorphous alloy which shows superior soft magnetic properties.<sup>26,27</sup> Since metallic glass is widely used for sensor applications, thin film form of this material would be of great interest for integrating thin film sensors with today's microelectronics. This can be realized by depositing thin films of this material on suitable substrates. Previous attempts for preparing thin film of this material by thermal evaporation showed that the composition of the films was rich in Fe and Ni and was depleted in Mo and B. Further, it was noticed that the magnetic properties are strongly dependent on the microstructure.<sup>10</sup>

The surface evolution of a thin film under SHI irradiation will be an outcome of a competition between sputtering induced surface roughening process and the material transport induced smoothing process. The final film morphology thus depends on the dominant process. Mayr and Averbach<sup>28</sup> observed that the smoothing of a rough amorphous film occurred during ion beam irradiation and radiation induced viscous flow was identified as the dominant surface relaxation mechanism. Mieskes *et al.*<sup>29</sup> observed an increase in surface roughness in Au, Zr, and Ti when irradiated with 230 MeV Au ions. The increased surface roughness was attributed to the sputtering induced by SHIs. The magnetic properties of thin films are strongly dependent on the surface/interface roughness and the SHI is an effective tool in modifying the surface of a material.

Considering the prospects of fabricating thin films based on Fe–Ni from metallic glass ribbons by simple vacuum evaporation techniques and the fact that amorphous alloys are not resistant to irradiation induced damages, a detailed investigation in probing the surface modification of amorphous thin films of Fe–Ni is worthwhile. It was thought that SHIs would modify the surface structure of these alloys and will eventually lead to modification of magnetic properties. Further, the studies related to SHI induced surface modifications and the intrinsic magnetic properties of thin films are rather scarce or seldom reported. The impingement of ions with different fluences on the alloy is bound to produce systematic microstructural changes and if these changes produce a pattern, this could effectively be used for tailoring the coercivity of these materials. The *in situ* method of tailoring coercivity using SHI is thus an ingenious tool in creating surface modification which will eventually lead to changes in the magnetic properties. Atomic force microscopy (AFM) is a promising tool for such a study on ion bombarded films where a minimum sample preparation is required. It offers a good lateral resolution too. The present study was carried out in order to investigate the effect of SHI irradiation on the magnetic and surface properties of Fe–Ni based amorphous alloys. Attempts are made to correlate the observed magnetic properties with surface evolution.

## II. EXPERIMENT

Fe–Ni films with a thickness of 35 nm were deposited using a composite target having the composition Fe<sub>40</sub>Ni<sub>38</sub>Mo<sub>8</sub>B<sub>14</sub> (METGLAS 2826) onto ultrasonically cleaned glass substrates employing thermal evaporation techniques. During deposition the base pressure in the chamber was maintained at  $1 \times 10^{-5}$  mbar with the help of a diffusion pump backed with a rotary pump. These samples were irradiated by 108 MeV Ag<sup>8+</sup> ions at room temperature with different fluences ranging from  $1 \times 10^{12}$  to  $3 \times 10^{13}$  ions cm<sup>-2</sup> using a 15 UD Pelletron accelerator at Inter University Accelerator Centre, New Delhi, India. A uniform irradiation over an area of  $1 \times 1$  cm<sup>2</sup> was achieved using a raster scanner. With the computer code SRIM, the nuclear stopping power  $(dE/dx)_n$ , the electronic stopping power  $(dE/dx)_e$ , and the residual range  $R_p$  were calculated as a function of ion energy. The value of  $(dE/dx)_e$  is close to 28 keV/nm and is

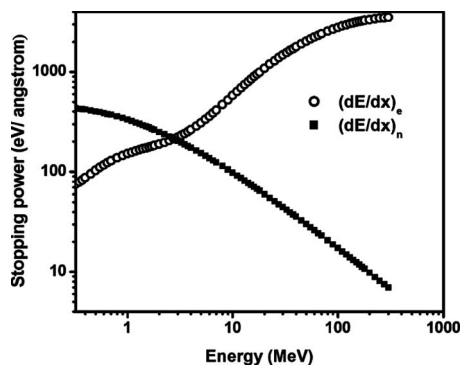


FIG. 1. SRIM simulation for calculating electronic and nuclear energy loss for 108 MeV  $\text{Ag}^{8+}$  ions in Fe–Ni target.

greater than the corresponding  $(dE/dx)_n$  values (1.6 eV/nm) (Fig. 1). The projected range of 108 MeV silver ions ( $R_p = 7 \mu\text{m}$ ) is higher than the film thickness so that the ion beam traverses through the material thickness and finally gets deposited in the substrate.

Transmission electron microscopy (TEM) experiments were carried out in a Joel JEM-2200 FS electron microscope operated at 200 kV. The films were subjected to XRD at grazing incidence using Bruker AXS diffractometer.  $\text{Cu } K\alpha$  with wavelength of 1.54 Å was employed for XRD measurements at a glancing angle of  $2^\circ$ . The scanning speed was adjusted to  $1^\circ/\text{min}$ . The surface morphology of pristine as well as irradiated films was examined using an atomic force microscope (Digital Instruments Nanoscope II). Room temperature magnetization measurements were carried out using a vibrating sample magnetometer (VSM) (DMS 1660) with an external field varying from  $-3$  to  $+3$  kOe.

### III. RESULTS

#### A. Composition of the film

The detailed x-ray photoelectron spectroscopy and energy dispersive x-ray spectroscopy studies on the pristine thin films showed that the films had the composition  $\text{Fe}_{55}\text{Ni}_{45}$ . The details are published elsewhere.<sup>10</sup>

#### B. TEM and glancing angle XRD studies

TEM observations were carried out on pristine thin films. The bright field image of the pristine Fe–Ni thin film is shown in Fig. 2(a). The microstructure exhibits a contrast typical of an amorphous material. The electron diffraction pattern [Fig. 2(b)] consists of a wide diffraction ring which is characteristic of an amorphous material. Glancing angle XRD (GAXRD) studies showed that both pristine and irradiated samples are amorphous in nature. The GAXRD pattern of pristine and irradiated films is depicted in Fig. 3. The amorphous nature of these films is clearly evident from these studies.

#### C. AFM studies

The surface topography of pristine and irradiated Fe–Ni thin films is shown in Fig. 4. It can be observed that there is a marked difference in the surface morphology of pristine

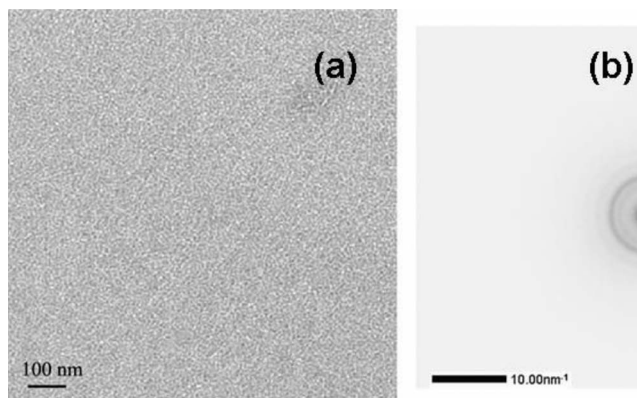


FIG. 2. (a) TEM bright field image of pristine thin films (b) corresponding electron diffraction pattern.

and irradiated films. The best known parameter in characterizing the morphology of a surface is the rms roughness ( $\rho_{\text{rms}}$ ), which expresses the variation in the height function  $h(r, t)$  over a two-dimensional substrate with linear size  $L$ .

$\rho_{\text{rms}} = \sqrt{\frac{1}{L^2} \sum [h(r, t) - \bar{h}(t)]^2}$ , where  $r$  is the position vector and the mean height is given by  $\bar{h}(t) = \frac{1}{L^2} \sum h(r, t)$ . The rms roughness was calculated for both pristine as well as irradiated films and was depicted in Fig. 5 as a function of fluence. It is clear that roughness increases with increase in ion fluence.

#### D. VSM studies

Figure 6 shows the hysteresis loop for pristine and irradiated films measured with the applied field parallel to the film plane. It can be noticed that the coercivities for pristine and irradiated films are different. The variation in coercivity with fluence is plotted and is depicted in Fig. 7. The squareness ratios ( $M_r/M_s$ ) for pristine and samples irradiated with SHIs at various fluences of  $1 \times 10^{12}$ ,  $3 \times 10^{12}$ , and  $3 \times 10^{13}$  ions/cm<sup>2</sup> are 0.75, 0.67, 0.50, and 0.44. It is clear that the squareness decreases with increase in the ion fluence.

### IV. DISCUSSIONS

GAXRD studies showed that both pristine and irradiated films are amorphous. It is to be noted that Rizza *et al.*<sup>30</sup> observed a crystallization phenomena in  $\text{Fe}_{73.5}\text{Nb}_4\text{Cr}_5\text{Cu}_1\text{B}_{16}$  and  $\text{Fe}_{90}\text{Zr}_7\text{B}_3$  meltspun ribbons. The nonobservance of such a phenomena in the present case can be due to following reasons. Ion fluence in the present case ( $\sim 10^{13}$  ions/cm<sup>2</sup>) is high so that it may be above a critical fluence. Assuming that  $1 \leq S_e/S_{\text{th}} \leq 2.7$ , the ion track radii can be approximated as  $R_e^2 = \ln S_e$ .<sup>31</sup> Here  $R_e$  is the track radius,  $S_e$  is the electronic energy loss, and  $S_{\text{th}}$  is the threshold energy for track formation. The approximate value of  $R_e$  in the present study is  $\sim 1.8$  nm. Since the estimated track diameter is  $\sim 3.6$  nm, the  $1 \text{ cm}^2$  sample will be fully covered with ion tracks at a fluence of about  $1 \times 10^{13}$ , corresponding to  $1/\pi R_e^2$ . Therefore there will be a considerable overlapping of tracks at  $3 \times 10^{13}$  ions/cm<sup>2</sup>. The impinging ions may overlap and therefore there will be an enhanced probability for reamorphization or sputtering of the crystallites formed if any. The

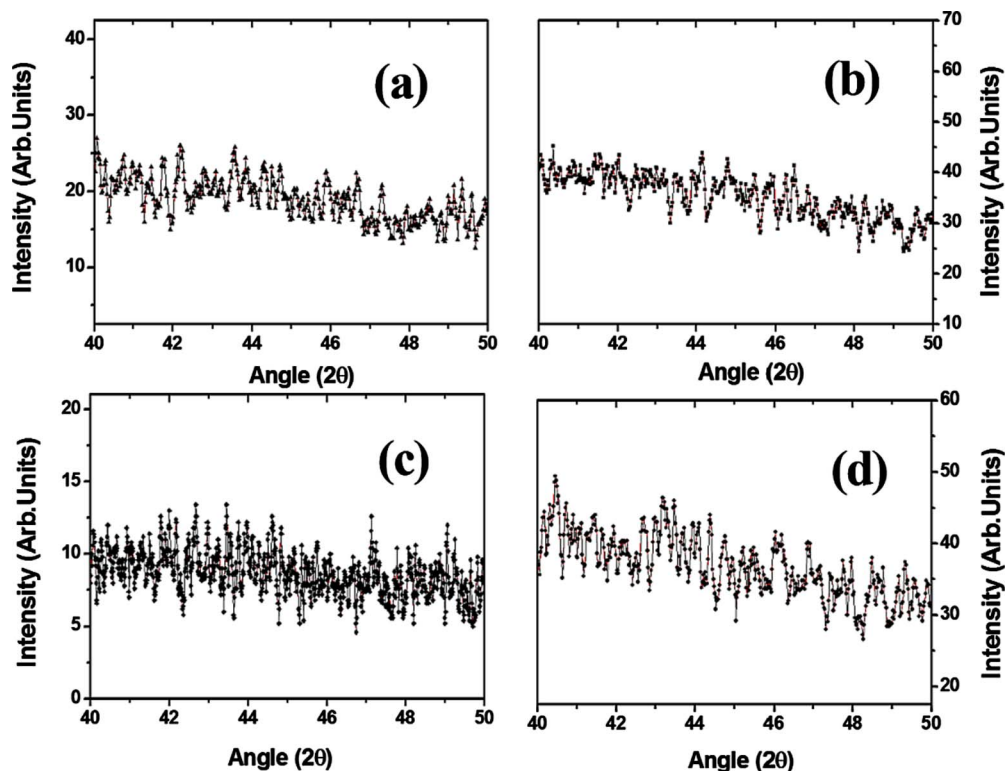


FIG. 3. (Color online) GAXRD pattern for (a) pristine and irradiated films with fluences of (b)  $1 \times 10^{12}$ , (c)  $3 \times 10^{12}$ , and (d)  $3 \times 10^{13}$  ions/cm<sup>2</sup>.

chemical composition is different in the present work [rich in Fe, Ni, and deficient in metalloids (B and Mo)]. It has been previously reported that the local composition plays a major role in stabilizing or destabilizing the amorphous structure upon SHI bombardment.<sup>30</sup> Also in the previous work the ion energy was in the GeV regime and linear electronic energy deposition in the present work is low ( $\sim 28$  keV/nm) when compared to the previous work ( $\sim 45$  keV/nm).<sup>30</sup> Regardless of roughness variation, AFM images show that the lateral size of the surface features increases with ion fluence and at  $3 \times 10^{13}$  ions/cm<sup>2</sup> the size decreases. Ion beam irradiation is known to increase the adatom diffusivity.<sup>32</sup> It is clear from AFM images that the pristine sample itself has some irregularities on the surface with an average height of  $\sim 0.6$  nm. The diffusing atoms can be trapped by these irregularities resulting in the accumulation of adatoms. This results in an increase in the lateral size with ion beam irradiation. It is also to be noted that the estimated fluence for track overlapping is  $\sim 1 \times 10^{13}$  ions/cm<sup>2</sup>. The reduction in lateral size at  $3 \times 10^{13}$  could be due to the fragmentation of surface structures as a result of multiple ion impacts on the surface.

The topographical evolution of a solid surface during ion beam irradiation is governed by the interplay between the dynamics of surface roughening that occurs due to sputtering and smoothing induced by material transport during surface diffusion. The increased surface roughness with fluence implies that the roughening process is predominant here.

The SHI induced roughening of Fe–Ni surfaces is in accordance with the expectation of an inelastic thermal spike model. According to this model, during the passage of the SHI a large amount of energy is deposited in the electronic

system of the solid and is transferred to the atoms by electron-phonon interaction. The first step in this process is the electronic excitation and ionization along the track of the projectile (within less than  $10^{-16}$  s). The heat transfer from electronic to atomic subsystem becomes substantial between  $10^{-14}$  and  $10^{-12}$  s depending on the magnitude of the coupling between both subsystems. After about  $10^{-10}$  s the region virtually cools down to ambient temperatures.

Temperature of the thermal spikes thus generated depends on (a) the volume in which the energy imparted by the SHIs diffuses due to the mobility of the hot electron gas and (b) the strength of the electron-phonon coupling that determines the efficiency of the transfer of the energy from the electronic system to the lattice. Depending on the amount of energy transferred to the atomic system and the attained temperature, specific phase changes can be induced such as transitions from the solid to liquid phase or liquid to vapor phase. Surface roughening is assumed to be because of the evaporation of atoms from a hot surface heated by an inelastic thermal spike. This gives credence to the hypothesis that SHI induced sputtering plays a predominant role in the surface roughening process of Fe–Ni thin films.

Similar increase in surface roughness with an increase in ion fluence was also observed by Mieskes *et al.*<sup>29</sup> in gold, zirconium, and titanium metals. In their work Au, Zr, and Ti metals irradiated with 230 MeV Au ions exhibited an increase in surface roughness with ion fluence. In the case of Ti the rms roughness increased from 100 nm to 1  $\mu$ m range when the ion fluence was increased from  $2 \times 10^{14}$  to  $1 \times 10^{15}$  ions/cm<sup>2</sup>. The increased surface roughness was attributed to the SHI induced sputtering and the combined

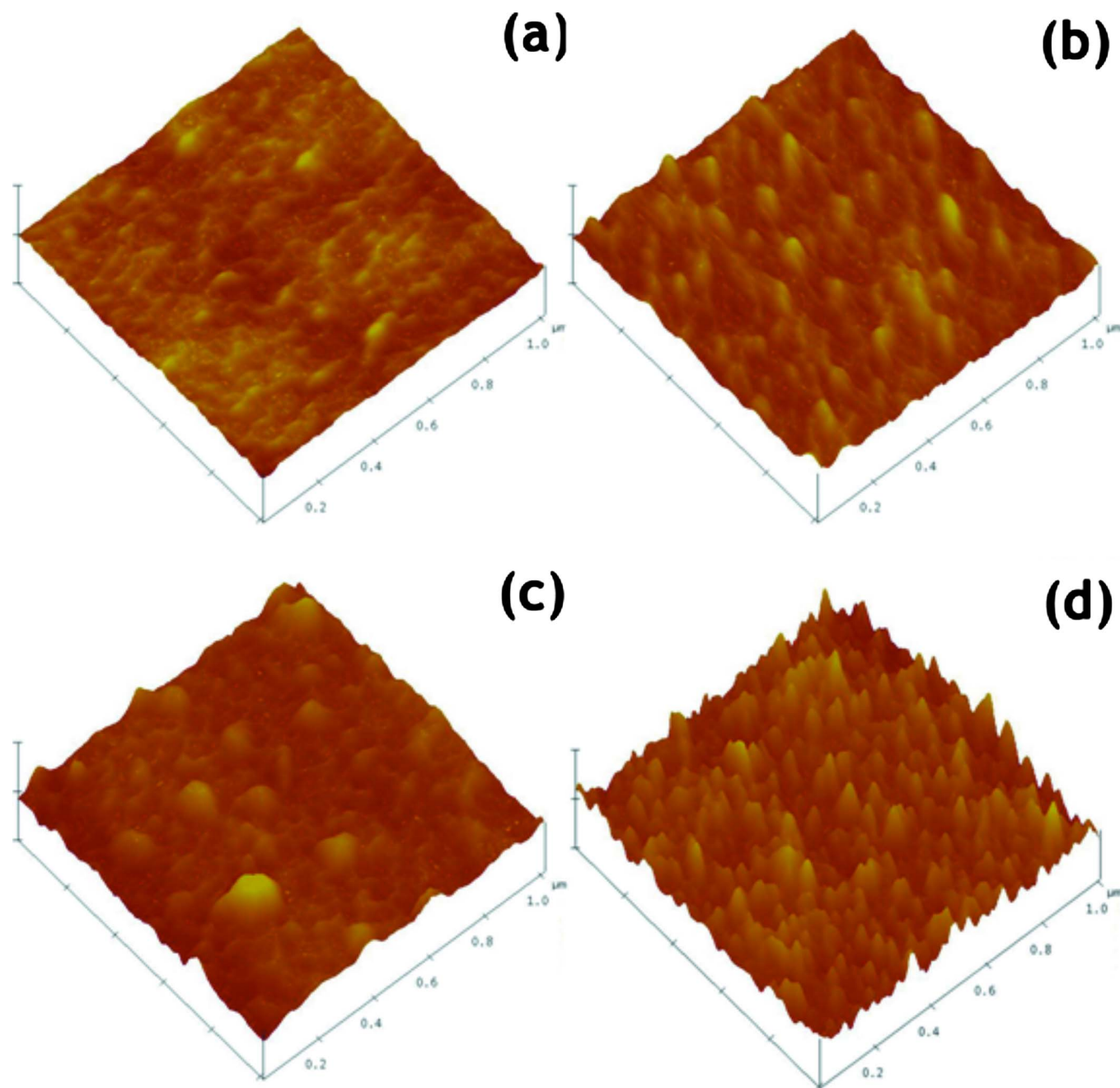


FIG. 4. (Color online) AFM images for (a) pristine and irradiated films with fluences of (b)  $1 \times 10^{12}$ , (c)  $3 \times 10^{12}$ , and (d)  $3 \times 10^{13}$  ions/cm<sup>2</sup> ( $x$  scale  $0.2 \mu\text{m}/\text{division}$ ,  $z$  scale  $20 \text{ nm}/\text{division}$ ).

electronic and nuclear heating effect contributed to the sputtering yield and was explained using an extended thermal spike model.

The observed coercivity changes can be correlated with the surface evolution of the films with SHI irradiation. It is known that surface topography only affects the magnetic properties of the surface region within 10–20 nm depth.<sup>33</sup> Hence surface techniques such as magneto-optic Kerr effect bring about a better correlation between the surface morphology and magnetic properties because of their surface sensitivity.<sup>34</sup> However it is to be noted that the thickness of the films in the present study is  $\sim 35$  nm and though VSM is a bulk technique, the hysteresis loop traced by the VSM represents the surface effects due to the limited thickness of

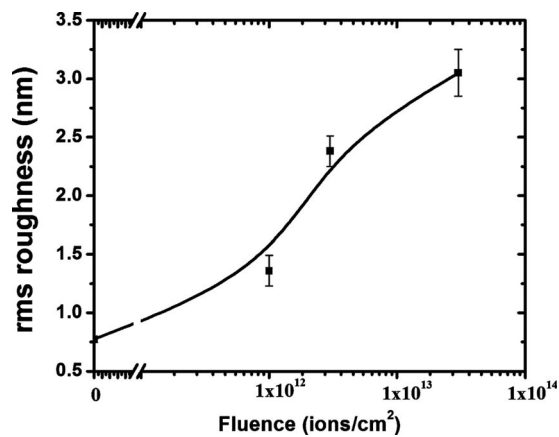


FIG. 5. Variation in rms roughness with ion fluence.

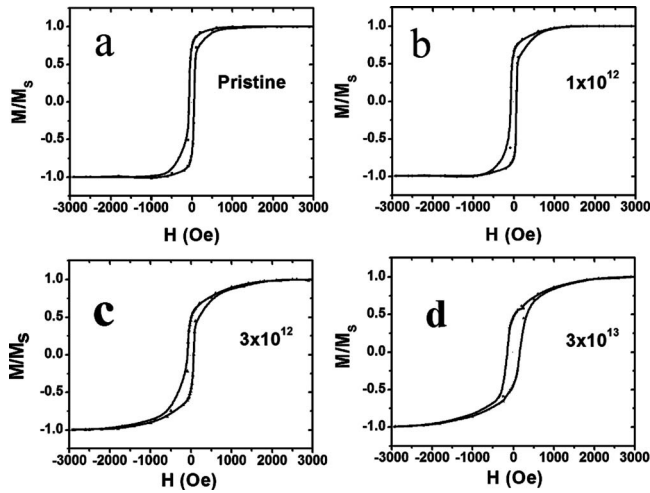


FIG. 6. Room temperature hysteresis loops for (a) pristine and irradiated films at fluences of (b)  $1 \times 10^{12}$ , (c)  $3 \times 10^{12}$ , and (d)  $3 \times 10^{13}$  ions/cm<sup>2</sup>.

the film. The coercive force is a measure of the magnetic field necessary to reduce the net magnetization of a ferromagnetic material from its saturation value in some selected direction to zero in that direction. The coercivity depends on the way in which the magnetization changes. There are two mechanisms by which this occurs: (a) by net magnetization rotation and (b) by domain wall motion. In soft magnetic materials the change in magnetization is primarily due to domain wall motion. Since this is a low energy process when compared to rotation of the net magnetization, the domain wall motion is associated with small coercive fields. Also it should be noted that pinning centers such as dislocations and grain boundaries are nonexistent in an amorphous alloy. So the possible mechanism for the increase in coercivity is the presence of surface pinning states. In the present case the changes in coercivity are entirely due to the modifications on the surface of the film and no other mechanisms (for example, nanocrystallization by heating effects of ion beams) are contributing to it. Very small irregularities on the surface of a film inhibit the passage of a domain wall because the energy stored within a domain wall surrounding such a region is smaller than that in an undisturbed domain wall and consequently the system energy must be increased to enable the domain wall motion. A possible mechanism involved in this surface pinning can be as follows. When the magnetiza-

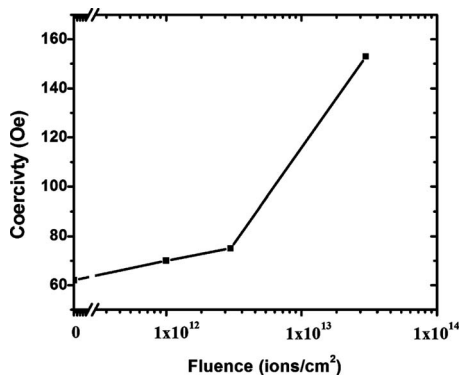


FIG. 7. Variation in coercivity with ion fluence.

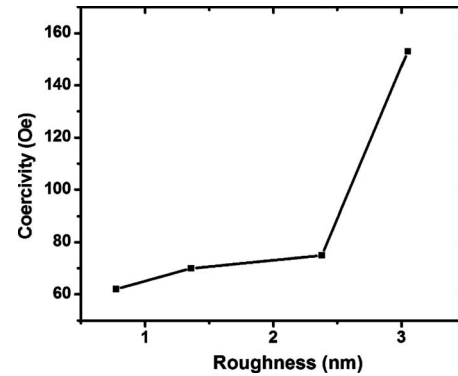


FIG. 8. Variation in coercivity with rms roughness.

tion within a domain wall intersects the surface, the magnetostatic energy is greater for surface regions which are normal to the domain wall than for those which are not. Consequently, the wall prefers irregular surface regions and may be pinned at such locations.<sup>35</sup>

From AFM images and data it is clear that the surface roughness increases with increase in ion fluence, and therefore more sites will be available for domain wall pinning and this resulted in an increased coercivity at higher ion fluences (see Fig. 8). The increase in the value of coercivity with an increase in surface roughness is in line with observation of other researchers.<sup>36–38</sup> Li *et al.*<sup>36</sup> studied the magnetization reversal process of Co film deposited on plasma etched Si substrates. The increased coercivity was attributed to the contribution of domain wall pinning in the magnetization reversal mechanism. Doherty *et al.*<sup>37</sup> observed an increase in coercivity with increased surface roughness in magnetic multilayer systems. They explained that roughness caused a discontinuity in the magnetization at the surface, which in turn created a self-pinning field due to induced surface or interface magnetic poles. Swerts *et al.*<sup>38</sup> studied the magnetization reversal mechanism and coercivity in 30 nm Fe films deposited on Ag buffer layers having different surface roughnesses. They observed that coercivity increases with an increase in surface roughness and the magnetization reversal process is influenced by the surface roughness. The increase in coercivity with an increase in surface roughness found in the Fe–Ni amorphous alloy is in agreement with the findings of these researchers. The observed decrease in squareness with increase in ion fluence is due to the increase in the in-plane demagnetization factor with an increase in surface roughness.<sup>39</sup> Roughness induced local in-plane magnetic poles results in nonuniform response of spins to an applied magnetic field.<sup>40</sup> This increases the saturating field for samples irradiated at higher fluences. Though SHI irradiation deteriorates the soft magnetic properties of the films, the increased coercivity and reasonable remanence ( $\sim 0.5$ ) suggest that a judicious choice of the fluence can alter the magnetic characteristics which suits novel applications of magnetic thin films. For example, there is intense interest, for data storage applications, in patterned magnetic media; in such media magnetic “contrast” is required at periodic intervals. This contrast can be obtained by alternate soft and hard magnetic regions by subjecting selected areas to SHI irradiation.

Present study demonstrates that SHI is an effective tool in modifying the surface morphology of a magnetic thin film. This property can be used for controlling useful magnetic properties such as coercivity.

## V. CONCLUSIONS

In conclusion, it was found that bombardment of 108 MeV Ag<sup>8+</sup> ions can result in roughening of Fe–Ni based amorphous thin film surfaces. The ion irradiation induced roughening can be due to the sputtering phenomena exhibited as a result of high electronic energy deposition. The coercivity of these films was found to increase with an increase in ion fluence. The increased coercivity is due to the increased surface roughness which provides pinning sites for inhibiting domain wall motion. These results are promising and can be useful in tailoring the magnetic properties of a magnetic material in a controlled fashion.

## ACKNOWLEDGMENTS

This work was supported by Inter University Accelerator Centre New Delhi, India through UGC Funded University Project (UFUP) under Grant No. 35306. We also thank Jai Prakash, Y. K. Mishra, and S. Mohapatra for their help during ion beam irradiation. We also wish to thank Pelletron group at IUAC, New Delhi for their help during the ion beam experiment. S.T. acknowledges CSIR, New Delhi for senior research fellowship.

<sup>1</sup>E. Komova, M. Varga, R. Varga, P. Vojtanik, J. Bednarcik, J. Kovac, M. Provencio, and M. Vazquez, *Appl. Phys. Lett.* **93**, 062502 (2008).

<sup>2</sup>J. P. Chu, C.-T. Lo, Y.-K. Fang, and B.-S. Han, *Appl. Phys. Lett.* **88**, 012510 (2006).

<sup>3</sup>S. X. Wang, N. X. Sun, M. Yamaguchi, and S. Yabukami, *Nature (London)* **407**, 150 (2000).

<sup>4</sup>R. Hasegawa, *Mater. Sci. Eng., A* **375–377**, 90 (2004).

<sup>5</sup>M. E. McHenry, M. A. Willard, and D. E. Laughlin, *Prog. Mater. Sci.* **44**, 291 (1999).

<sup>6</sup>R. Alben, J. J. Becker, and M. C. Chi, *J. Appl. Phys.* **49**, 1653 (1978).

<sup>7</sup>T. R. Anantharaman, *Metallic Alloys Production Properties and Applications* (Trans Tech, Aedermannsdorf, 1984), p. 2.

<sup>8</sup>M. Vopsaroiu, M. Georgieva, P. J. Grundy, G. Vallejo Fernandez, S. Manzoor, and M. J. Thwaites, *J. Appl. Phys.* **97**, 10N303 (2005).

<sup>9</sup>S. Ladak, L. E. Fernández-Outón, and K. O'Grady, *J. Appl. Phys.* **103**, 07B514 (2008).

<sup>10</sup>S. Thomas, S. H. Al-Harhi, D. Sakthikumar, I. A. Al-Omari, R. V. Ramanujan, Y. Yoshida, and M. R. Anantharaman, *J. Phys. D* **41**, 155009 (2008).

<sup>11</sup>Y.-P. Zhao, R. M. Gamache, G.-C. Wang, T.-M. Lu, G. Palasantzas, and J. Th. M. De Hosson, *J. Appl. Phys.* **89**, 1325 (2001).

<sup>12</sup>Y.-P. Zhao, G. Palasantzas, G.-C. Wang, and J. Th. M. De Hosson, *Phys. Rev. B* **60**, 1216 (1999).

<sup>13</sup>D. Paramanik, A. Pradhan, and S. Varma, *J. Appl. Phys.* **99**, 014304 (2006).

<sup>14</sup>S. Mechler, C. Abromeit, N. Wanderka, M.-P. Macht, T. Zunkley, G. Schumacher, and S. Klaumünzer, *Nucl. Instrum. Methods Phys. Res. B* **245**, 133 (2006).

<sup>15</sup>S. Nagata, S. Higashi, B. Tsuchiya, K. Toh, T. Shikama, K. Takahiro, K. Ozaki, K. Kawatusra, S. Yamamoto, and A. Inouye, *Nucl. Instrum. Methods Phys. Res. B* **257**, 420 (2007).

<sup>16</sup>G. Rizza, A. Dunlop, and M. Kopcewicz, *Nucl. Instrum. Methods Phys. Res. B* **245**, 130 (2006).

<sup>17</sup>P. Ziemann, W. Miehle, and A. Plewnia, *Nucl. Instrum. Methods Phys. Res. B* **80–81**, 370 (1993).

<sup>18</sup>E. M. Bringa and R. E. Johnson, *Phys. Rev. Lett.* **88**, 165501 (2002).

<sup>19</sup>R. L. Fleischer, P. B. Price, R. M. Walker, and E. L. Hubbard, *Phys. Rev.* **156**, 353 (1967).

<sup>20</sup>R. L. Fleischer, P. B. Price, and R. M. Walker, *J. Appl. Phys.* **36**, 3645 (1965).

<sup>21</sup>S. Klaumünzer and G. Schumacher, *Phys. Rev. Lett.* **51**, 1987 (1983).

<sup>22</sup>G. Schumacher, S. Klaumünzer, S. Rentzsch, and G. Vogl, *J. Non-Cryst. Solids* **61–62**, 565 (1984).

<sup>23</sup>A. Audouard, R. Mamy, M. Toulemonde, G. Szenes, and L. Thomé, *Europhys. Lett.* **40**, 527 (1997).

<sup>24</sup>A. Audouard, R. Mamy, M. Toulemonde, G. Szenes, and L. Thomé, *Nucl. Instrum. Methods Phys. Res. B* **146**, 217 (1998).

<sup>25</sup>A. Dunlop, G. Jaskierowicz, G. Rizza, and M. Kopcewicz, *Phys. Rev. Lett.* **90**, 015503 (2003).

<sup>26</sup>S. W. Du and R. V. Ramanujan, *J. Non-Cryst. Solids* **351**, 3105 (2005).  
<sup>27</sup>www.metglas.com

<sup>28</sup>S. G. Mayr and R. S. Averback, *Phys. Rev. Lett.* **87**, 196106 (2001).

<sup>29</sup>H. D. Mieskes, W. Assmann, F. Grüner, H. Kucal, Z. G. Wang, and M. Toulemonde, *Phys. Rev. B* **67**, 155414 (2003).

<sup>30</sup>G. Rizza, A. Dunlop, G. Jaskierowicz, and M. Kopcewicz, *Nucl. Instrum. Methods Phys. Res. B* **226**, 609 (2004).

<sup>31</sup>G. Szenes, *Phys. Rev. B* **51**, 8026 (1995).

<sup>32</sup>P. Bai, J. F. McDonald, T.-M. Lu, and M. J. Costa, *J. Vac. Sci. Technol. A* **9**, 2113 (1991).

<sup>33</sup>K. Zhang, M. Uhrmacher, H. Hofsäss, and J. Krauser, *J. Appl. Phys.* **103**, 083507 (2008).

<sup>34</sup>K. Zhang, F. Rotter, M. Uhrmacher, C. Ronning, J. Krauser, and H. Hofsäss, *New J. Phys.* **9**, 29 (2007).

<sup>35</sup>D. S. Rodbell and C. P. Bean, *Phys. Rev.* **103**, 886 (1956).

<sup>36</sup>M. Li, Y. P. Zhao, G. C. Wang, and H. G. Min, *J. Appl. Phys.* **83**, 6287 (1998).

<sup>37</sup>S. A. Doherty, J. G. Zhu, M. Dugas, S. Anderson, and J. Tersteeg, *IEEE Trans. Magn.* **34**, 840 (1998).

<sup>38</sup>J. Swerts, K. Temst, N. Vandamme, C. Van Haesendonck, and Y. Bruynseraede, *J. Magn. Mater.* **240**, 380 (2002).

<sup>39</sup>M. Li, G.-C. Wang, and H.-G. Min, *J. Appl. Phys.* **83**, 5313 (1998).

<sup>40</sup>D. Aurongzeb, K. Bhargava Ram, and L. Menon, *Appl. Phys. Lett.* **87**, 172509 (2005).